8-27-2001

Evaluation of uncertainties in regional climate change simulations

Z. Pan
Iowa State University

J. H. Christensen
Danish Meteorological Institute

R. W. Arritt
Iowa State University, rwarritt@iastate.edu

W. J. Gutowski Jr.
Iowa State University, gutowski@iastate.edu

E. S. Takle
Iowa State University, gstakle@iastate.edu

See next page for additional authors

Evaluation of uncertainties in regional climate change simulations

Abstract

We have run two regional climate models (RCMs) forced by three sets of initial and boundary conditions to form a 2×3 suite of 10-year climate simulations for the continental United States at approximately 50 km horizontal resolution. The three sets of driving boundary conditions are a reanalysis, an atmosphere-ocean coupled general circulation model (GCM) current climate, and a future scenario of transient climate change. Common precipitation climatology features simulated by both models included realistic orographic precipitation, east-west transcontinental gradients, and reasonable annual cycles over different geographic locations. However, both models missed heavy cool-season precipitation in the lower Mississippi River basin, a seemingly common model defect. Various simulation biases (differences) produced by the RCMs are evaluated based on the 2×3 experiment set in addition to comparisons with the GCM simulation. The RCM performance bias is smallest, whereas the GCM-RCM downscaling bias (difference between GCM and RCM) is largest. The boundary forcing bias (difference between GCM current climate driven run and reanalysis-driven run) and intermodel bias are both largest in summer, possibly due to different subgrid scale processes in individual models. The ratio of climate change to biases, which we use as one measure of confidence in projected climate changes, is substantially larger than 1 in several seasons and regions while the ratios are always less than 1 in summer. The largest ratios among all regions are in California. Spatial correlation coefficients of precipitation were computed between simulation pairs in the 2×3 set. The climate change correlation is highest and the RCM performance correlation is lowest while boundary forcing and intermodel correlations are intermediate. The high spatial correlation for climate change suggests that even though future precipitation is projected to increase, its overall continental-scale spatial pattern is expected to remain relatively constant. The low RCM performance correlation shows a modeling challenge to reproduce observed spatial precipitation patterns.

Disciplines

Atmospheric Sciences | Climate

Comments

This article is from *Journal of Geophysical Research: Atmospheres* 106 (2001): 17735–17751, doi:10.1029/2001JD900193. Posted with permission.

Authors

Z. Pan, J. H. Christensen, R. W. Arritt, W. J. Gutowski Jr., E. S. Takle, and F. Otieno

JOURNAL OF GEOPHYSICAL RESEARCH, VOL. 106, NO. D16, PAGES 17,735–17,751, AUGUST 27, 2001

Evaluation of uncertainties in regional climate change simulations

Z. Pan,[1] J. H. Christensen,[2] R. W. Arritt,[1] W. J. Gutowski Jr.,[1,3]
E. S. Takle, [1,3] and F. Otieno[3]

Abstract. We have run two regional climate models (RCMs) forced by three sets of initial and boundary conditions to form a 2x3 suite of 10-year climate simulations for the continental United States at approximately 50 km horizontal resolution. The three sets of driving boundary conditions are a reanalysis, an atmosphere-ocean coupled general circulation model (GCM) current climate, and a future scenario of transient climate change. Common precipitation climatology features simulated by both models included realistic orographic precipitation, east-west transcontinental gradients, and reasonable annual cycles over different geographic locations. However, both models missed heavy cool-season precipitation in the lower Mississippi River basin, a seemingly common model defect. Various simulation biases (differences) produced by the RCMs are evaluated based on the 2x3 experiment set in addition to comparisons with the GCM simulation. The RCM performance bias is smallest, whereas the GCM-RCM downscaling bias (difference between GCM and RCM) is largest. The boundary forcing bias (difference between GCM current climate driven run and reanalysis-driven run) and intermodel bias are both largest in summer, possibly due to different subgrid scale processes in individual models. The ratio of climate change to biases, which we use as one measure of confidence in projected climate changes, is substantially larger than 1 in several seasons and regions while the ratios are always less than 1 in summer. The largest ratios among all regions are in California. Spatial correlation coefficients of precipitation were computed between simulation pairs in the 2x3 set. The climate change correlation is highest and the RCM performance correlation is lowest while boundary forcing and intermodel correlations are intermediate. The high spatial correlation for climate change suggests that even though future precipitation is projected to increase, its overall continental-scale spatial pattern is expected to remain relatively constant. The low RCM performance correlation shows a modeling challenge to reproduce observed spatial precipitation patterns.

1. Introduction

Over the past decade or so there have been numerous modeling studies on global warming [e.g., *Gates et al.*, 1999; *Houghton et al.*, 1996]. Public awareness of global-scale changes, such as global warming and environmental deterioration, has brought interest in projecting global climate changes onto local or regional scales where social and economic impacts may be evaluated. However, present-day computational resources needed for multidecadal global change simulation limit the spatial resolution of global climate models (GCM) to scales (200-300 km) larger than those needed for impacts analysis.

[1] Department of Agronomy, Iowa State University, Ames.
[2] Danish Meteorological Institute, Copenhagen, Denmark.
[3] Department of Geological and Atmospheric Sciences, Iowa State University, Ames.

Paper number 2001JD900193.
0148-0227/01/2001JD900193$09.00

Statistical downscaling has been widely used as a computationally inexpensive method for projecting GCM results to local scales [*Karl et al.*, 1990; *Zorita et al.*, 1995; *Cubasch et al.*, 1996]. An alternative downscaling method, dynamic downscaling by nesting a regional climate model (RCM) into a GCM, was pioneered by *Dickinson et al.* [1989] and *Giorgi et al.* [1992]. Although computationally demanding, this approach has become a major tool in regional climate studies due to rapid advances in computer power and constant refinement in numerical techniques. The RCM approach has been applied for Europe [e.g., *Cress et al.*, 1995; *Jones et al.*, 1995; *Podzun et al.*, 1995; *Christensen et al.*, 1997, 1998], for North America [Giorgi *et al.*, 1994; *Leung and Ghan*, 1999], for Australia [*McGregor and Walsh*, 1994], for Africa [*Semazzi et al.*, [1993], and for Asia [*Hirakuchi and Giorgi*, 1995; *Leung et al.*, 1999].

Climate simulation is known to be model dependent, although GCM simulations have shown less intermodel bias for North America than for most other regions of the world [*Houghton et al.*, 1996]. *Machenhauer et al.* [1998] has reported the only published multiple year intercomparison project that used regional models. These simulations covered

a common area (Europe) and period, but the lateral boundary conditions, integration duration, and simulation domain size were only loosely controlled. The Project to Intercompare Regional Climate Simulations has more strictly defined integration period and domain size, but simulations to date have covered only 60 days [*Takle et al.*, 1999].

Over the United States, all multiyear regional climate simulations that have been attempted used a single RCM. The longest regional model simulations previously reported for the continental United States have been 3 years for analysis-driven simulations [*Giorgi et al.*, 1994; *Giorgi and Shields*, 1999] and 5 years for simulations driven by GCM output [*Giorgi et al.*, 1998]. Somewhat longer simulations have been performed for subcontinental portions of the United States [e.g., *Leung and Ghan*, 1999]. By one-way nesting a regional climate model to a GCM *Giorgi et al.* [1994] showed the RCM's general improvement over the corresponding GCM for a 3.5-year simulation. The projected $2xCO_2$ warming was close between the GCM and RCM, but projected precipitation change differed not only in magnitude but also in sign. Using another regional model, *Leung and Ghan* [1999] also showed significant differences between the RCM and GCM in projecting the $2xCO_2$ scenario climate. However, their projected precipitation change under $2xCO_2$ climate had a dipole structure in the western United States, quite different from the results of *Giorgi et al.* [1994] which showed overwhelming precipitation increase along the Pacific Coast. It is not clear whether the difference comes from different RCM model internal parameterizations, GCM forcing lateral boundary conditions, or simulation domains and integration time periods and duration since all of these differed between the two studies.

These intermodel differences indicate a need to analyze RCM precipitation climatology from multiple models so that we can evaluate the uncertainties of these climatologies. In the present paper, two regional climate models, RegCM2 [*Giorgi et al.*,1993a,1993b] and the Danish Meteorological Institute's HIRHAM [*Christensen et al.*, 1996], have been used to produce a suite of 10-year climate simulations for the continental United States at approximately 50 km horizontal grid spacing. Both RegCM and HIRHAM were run using three sets of driving boundary conditions: National Centers for Environmental Prediction (NCEP) reanalysis, Hadley Centre coupled atmosphere-ocean GCM (HADCM2) simulation of current climate, and a HADCM2 future scenario climate [*Johns et al.*, 1997].

The objectives of this paper are (1) to distinguish different types of simulation biases that are reflected in the previous independent, uncoordinated simulations, most of which are over different geographical locations and time periods, and (2) to evaluate climate change confidence by comparing projected changes with various biases identified in objective (1). In addition, as the first decadal, multimodel, transient U.S. regional climate simulation, this study will serve as a contrast to previous $2xCO_2$ RCM equilibrium runs.

2. Model and Experiment Configuration

2.1. RegCM2

RegCM2 [*Giorgi et al.*, 1993a, 1993b] incorporates the CCM2 radiation package [*Briegleb*, 1992] and the BATS version 1e [*Dickinson et al.* 1992] surface package. For this study, simulations used the modified *Grell* [1993] convection scheme. This mass flux scheme is a simplified version of Arakawa-Schubert convection [*Arakawa and Schubert*, 1974] that assumes a single updraft and downdraft. Large-scale precipitation was computed using a simple warm-cloud physics, explicit moisture scheme [*Hsie et al.*, 1984]. The model has a single cloud-water predictive variable. The turbulence parameterization uses the *Holtslag et al.* [1990] nonlocal scheme, which permits countergradient transport. The land surface scheme in RegCM2 has 18 categories of land use and 12 soil types. The model has three overlapping soil layers: top layer (10 cm), root zone (1-2 m depending on vegetation type), and deep soil (10 m). The model domain covered 101x75 grid points centered at (100°W, 37.5°N) with a horizontal grid spacing of 52 km. The vertical coordinate is $\sigma = (P - P_{top})/(P_{sfc} - P_{top})$, where p_{top} (=100 hPa) and p_{sfc} are pressure at the model top and the surface. The model in this study used 14 layers in the vertical, centered at σ=0.995, 0.980, 0.950, 0.895, 0.815, 0.720, 0.615, 0.510, 0.405, 0.300, 0.210, 0.135, 0.070, and 0.020. Model lateral boundary conditions were assimilated by nudging in a buffer zone of 15 grids [*Davies and Turner*, 1977]. The lateral boundary data were supplied by the reanalysis and GCM described in section 2.3 at 6-hour intervals and interpolated in time. The simulation domain and buffer zone were chosen so that westerly flow enters far from high mountains, which can produce large interpolation errors [*Hong and Juang*, 1998].

2.2. HIRHAM

The HIRHAM model used in this study is based on the adiabatic part of the HIRLAM short-range weather prediction model [*Källén*, 1996]. Replacement of the standard HIRLAM physical parameterization package with that of the general circulation model ECHAM4 [*Roeckner et al.*, 1996] has facilitated adaptation to long climate simulations [*Christensen et al.*, 1996]. The resulting model, HIRHAM4, has been further documented by *Christensen et al.* [1998]. Subgrid cumulus convection is parameterized by a mass flux scheme proposed by *Tiedtke* [1989]. In this scheme, three types of convection, shallow, midlevel, and penetrative, are defined, each of which has different closure assumptions. Simulation of large-scale precipitation follows the formulation developed by *Sundqvist* [1978], in which fractional cloud cover is based on grid-scale moisture content. The scheme has a predictive variable (cloud water) for liquid phase while ice phase is diagnosed. The atmospheric radiation scheme is taken from European Center for Medium-Range Weather Forecasts (ECMWF) model cycle 36 with addition of ozone, CFCs, and aerosols for climate simulations. The planetary boundary layer scheme is based on a local K type formulation. The land surface scheme uses 5 prognostic temperature layers and one (bucket) moisture layer. A zero flux lower boundary condition is applied for soil temperature. Runoff is calculated with the Arno scheme [*Dümenil and Todini*, 1988], which softens the onset of runoff by introducing a distribution of soil water holding capacities in the grid box, depending on orographic slope. A simple one-layer snow model is coupled to the land surface scheme [*DKRZ*, 1992; *Christensen et al.*, 1996]. Lateral boundary conditions are assimilated through nudging within a 10-grid nudging zone using a quasi-exponential function for most predictive variables similar to RegCM2. The discretization consists of 120x70 grid points with

horizontal grid spacing of 0.5° and 19 vertical levels in sigma-pressure hybrid coordinates [*Simmons* and *Burridge*, 1981] to the model top at 10 hPa. The model uses a rotated grid that places the equator in the middle of the domain. It should be noted that size of the domain and width of the forcing boundary zone are slightly different between the two RCMs because of their model domain configuration. This difference might affect the intermodel comparison, as will be discussed later.

2.3. Design of Experiments

Three sets of lateral boundary conditions were used to perform the simulations presented in this paper. The first simulation with "perfect" boundary conditions supplied by reanalyzed observational data sets offered the best available boundary conditions for which simulated results could be compared with observations. The other two simulations used results of a GCM as lateral boundary conditions for the RCMs.

2.3.1. Reanalysis driven run. The first run is driven by the NCEP reanalysis [*Kalnay et al.*, 1996] which provides buffer zone boundary conditions on a 28 sigma level Gaussian grid (1.875° latitude/longitude), for the period 1979-1988, coinciding with the Atmospheric Model Intercomparison Project (AMIP) experiments [*Gates et al.*, 1999]. The NCEP data were augmented by advanced very high resolution radiometer (AVHRR) retrievals of sea surface temperature (SST) from the Gulf of California and buoy observations of surface temperature in the North American Great Lakes.

2.3.2. HADCM2 current climate driven run. In our study, the GCM driving data for the current climate are from a HADCM2 control climate run. The fully coupled HADCM2 is one of the two atmosphere-ocean GCMs used for the U.S. National Assessment Project [*Doherty and Mearns*, 1999; *Sousounis*, 2000]. The HADCM2 is a finite difference model with horizontal grid spacing of 2.5° (latitude) x 3.75° (longitude), 19 vertical levels in the atmosphere, and 20 levels in the ocean. The HADCM2 control integration ran from 1860 to the 1990 (and beyond) with equivalent CO_2 fixed at 1990 level. The multi century integration was very stable with a negligible warming trend of only 0.016 K per century [*Johns et al.*, 1997]. The 10-year window selected corresponds roughly to 1990. The choice of 10-year window may have some effect on our results since 10 years is fairly short from a climatological perspective. We note that it would also have been desirable to perform a RCM simulation forced by a HADCM2 run that used only the atmospheric component of the GCM, forced by observed SSTs (similar to the approach of the AMIP [*Gates et al.*, 1999]). This would have provided an intermediate step between the reanalysis-driven RCM run and the run driven by the free-running coupled GCM. Such a run was not performed because such HADCM2 output was not available to us.

2.3.3. HADCM2 GHG scenario driven run. The HADCM2 output data used for our future scenario runs are from a transient simulation that assumed a 1% per year increase in effective greenhouse gases after 1990. Aerosol effects were not included in the HADCM2 transient GHG simulations used in this paper. Based on simulations with and without aerosol [e.g., *Roeckner et al.*, 1999], mean annual precipitation changes caused by the aerosol in the scenario climate of the United States are estimated to be ± 0.2 mm d^{-1} or less. The 10-year window selected corresponds to 2040-2049 for the scenario climate with CO_2 about 480 ppm. A slightly later 10-year window, say 2055-2064, would be a better choice as it would facilitate comparison with previous doubled CO_2 studies, but this time window was not available to us. The selection of any time slice from the GCM is arbitrary to a certain degree. Fortunately, the decadal-scale climate change as simulated by most GCMs is approximately linear in time since nonlinear changes tend to be smoothed when examining decadal scales. Furthermore, possible multiequilibrium modes do not persist on annual or longer timescales in ocean-atmosphere coupled models [*Tett et al.*, 1997]. Thus the choice of 10-year window may not greatly affect the subsequent RCM simulation.

2.3.4. Verifying observations. Observed precipitation was obtained from the Vegetation/Ecosystem Modeling and Analysis Project (VEMAP) [*Kittel et al.*, 1995] monthly precipitation archived on a 0.5°x0.5° grid for the period 1951-1990. We extracted the 10-year subset corresponding to the reanalysis simulation period, 1979-1988. Comparison of the 10-year period's observed precipitation (Figure 1a) with the climatology of the longer period shows very similar overall patterns, particularly over the western United States, reflecting terrain-forced precipitation. The largest difference is over the southeast United States where large-scale dynamic forcing frequently dominates. The overall precipitation during 1979-1988 is slightly smaller than the 40-year climatology (Figure 2a), partly due to the 1988 drought. Differences in precipitation between these two climate periods were smaller than the biases we discuss later. Our analysis is limited to the same region as the VEMAP archive, that is, the continental United States.

2.4. Definitions of Biases

We use the term "bias" to represent differences among various pairs of simulated precipitation fields and between simulated and observed fields. Some differences clearly are not biases in the strict sense, but for simplicity we use the term "bias" to refer to the entire set of comparisons. The following biases are defined from the 2x3 suite of RCM runs and corresponding GCM current climate simulations as part of a procedure for establishing a minimum confidence level for projected climate change in precipitation: (1) RCM performance bias, difference between reanalysis-driven RCM simulation and corresponding observations; (2) boundary forcing bias, difference between the RCM run driven by GCM current climate and the RCM run driven by reanalysis; (3) intermodel bias, difference between runs from different RCMs (HIRHAM minus RegCM2), both driven by reanalysis; (4) GCM-RCM downscaling bias, difference between the control GCM run and the corresponding RCM run driven by the GCM output, both for current climate.

The RCM performance bias depends on numerics, parameterization details, calibration choices, etc. of the individual models and measures model systematic errors and drift. Intermodel bias gives a range of RCM responses to external forcing, thereby indicating uncertainty in RCM simulations.

Boundary forcing bias represents the difference between RCM runs using the same model but forced by different boundary conditions. The reanalysis and the GCM control climate are not for the same 10-year period, since the

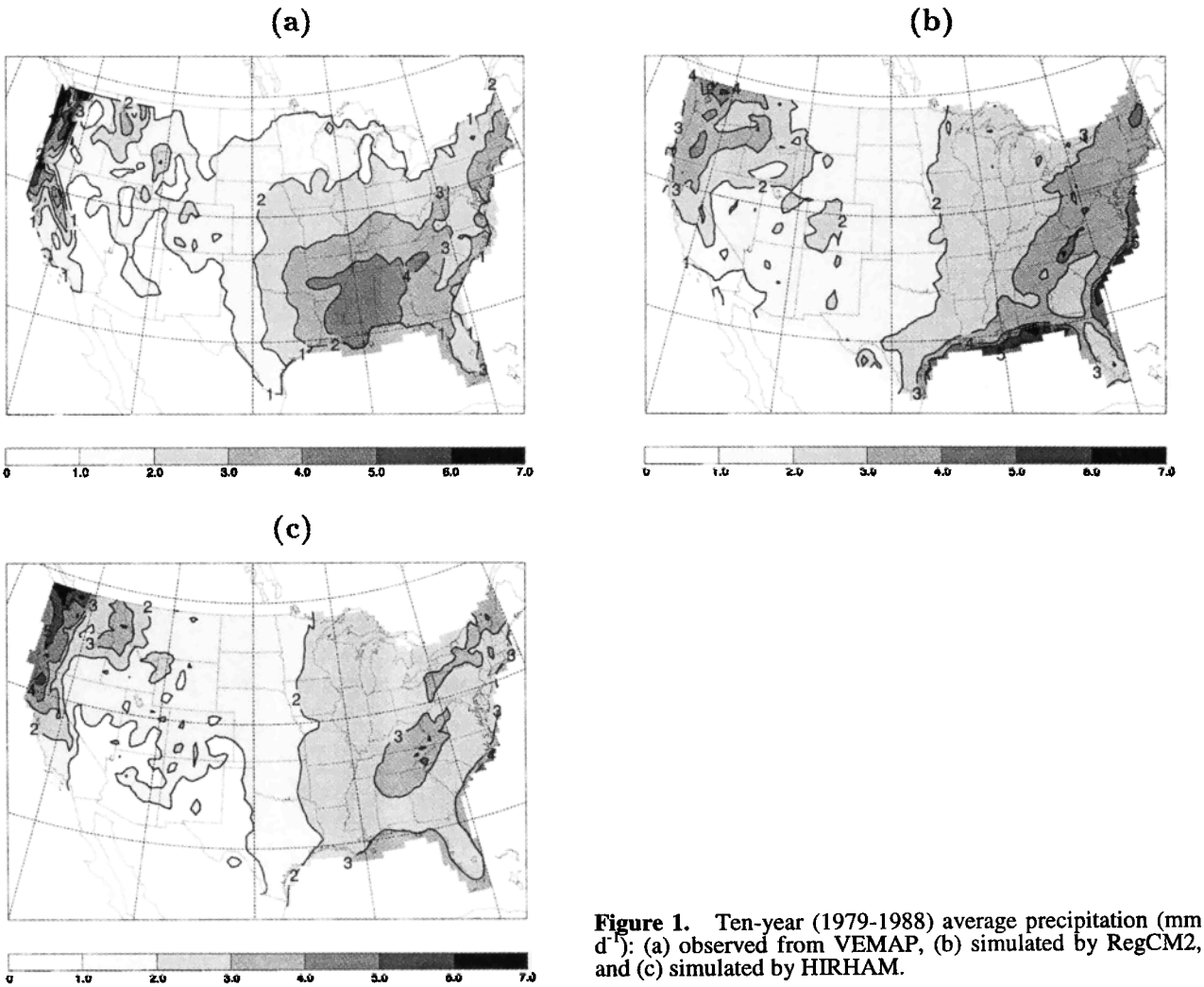

Figure 1. Ten-year (1979-1988) average precipitation (mm d^{-1}): (a) observed from VEMAP, (b) simulated by RegCM2, and (c) simulated by HIRHAM.

reanalysis-driven simulation covers the specific years 1979-1988, whereas the HADCM2 output is for an arbitrary 10-year window. The defined boundary forcing bias is meaningful in a statistical sense, assuming both represent current climatology. The only drawback is that the sample size (10 years) is relatively small, although this length is the longest integration to date for regional climate modeling of the continental United States.

The GCM-RCM downscaling bias indicates the disagreement in results between the RCM and GCM. It includes potential regional improvement that the RCM can add to the GCM, primarily by higher resolution, as well as errors attributable to the RCM.

Our intent here is not to search for causes of indicated biases but to present a methodology for classifying sources of uncertainty that undermine confidence in climate change simulation. We also compare these precipitation biases with climate change, defined to be the difference between RCM runs driven by the GCM scenario and control simulations. This comparison helps us address the question of whether or not RCM downscaling provides meaningful changes in regional precipitation on scales important for climate impact studies. Although we focus here on time-averaged precipitation, the methodology can be applied more broadly to analysis of other simulated fields.

2.5. Analysis Computations

All biases (ΔP) are based on 10-year averages over the complete annual cycle and over individual seasons: winter (December-January-February (DJF)), spring (March-April-May (MAM)), summer (June-July-August (JJA)), and fall (September-October-November (SON)). To account for spatial heterogeneity, biases are computed for specific regions. For example, RCM performance bias for a season in a region is given by

$$\Delta P_{\mathrm{RCM}} = \frac{\sum_{i=1}^{N} W_i (P_i^m - P_i^o)}{\sum_{i=1}^{N} W_i}, \qquad (1)$$

where P^O and P^m are time means of observed and model simulated precipitation, respectively, and N is the total number of grid points in the region as defined in section 4.1. W is a latitudinally dependent weight ($\cos\phi_i$), where ϕ_i is latitude of the i^{th} grid point. Model precipitation was first interpolated onto the VEMAP 0.5x0.5° grid, and then all statistics were computed as in (1) on the same grids for model and observed precipitation.

Regional bias measures the difference between two means but gives no information about spatial distribution. Two fields

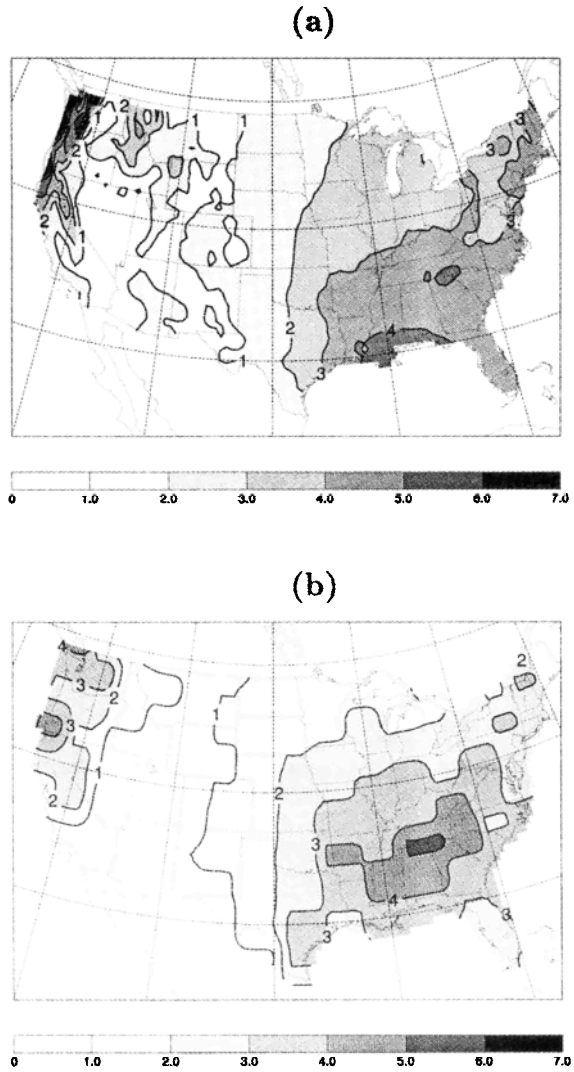

Figure 2. (a) VEMAP precipitation (mm d^{-1}) climatology for 1951-1990 and (b) 10-year average precipitation (mm d^{-1}) simulated by HADCM2 control run.

could have equal means but different spatial distribution. Thus we also compute coefficients of correlation in space between simulated and observed precipitation fields. For example, RCM (performance) correlation is

$$r_{RCM} = \frac{\dfrac{\sum_{i=1}^{N} W_i (P_i^o - \bar{P}^o)(P_i^m - \bar{P}^m)}{\sum_{i=1}^{N} W_i}}{\left[\dfrac{\sum_{i=1}^{N} W_i (P_i^o - \bar{P}^o)^2}{\sum_{i=1}^{N} W_i} \dfrac{\sum_{i=1}^{N} W_i (P_i^m - \bar{P}^m)^2}{\sum_{i=1}^{N} W_i} \right]^{1/2}}, \quad (2)$$

where an overbar represents the regional average.

We use the spatial standard deviation to represent spatial variance of precipitation and then compute the difference in spatial standard deviation as

$$\Delta\sigma_{RCM} = \left(\frac{\sum_{i=1}^{N} W_i (P^m{}_i - \bar{P}^m)^2}{\sum_{i=1}^{N} W_i} \right)^{1/2} - \left(\frac{\sum_{i=1}^{N} W_i (P^o{}_i - \bar{P}^o)^2}{\sum_{i=1}^{N} W_i} \right)^{1/2}. \quad (3)$$

The difference and spatial correlations due to boundary forcing, intermodel bias, GCM-RCM upscaling bias, and climate change are computed similarly.

3. Spatial and Seasonal Distribution of Differences

3.1. RCM Performance Bias

The observed annual precipitation climatology from VEMAP (Figure 1a) shows that the eastern United States is generally wet and the western United States is mostly dry but with heavy precipitation along the Pacific Northwest coast mainly because of winter storm tracks. Wetness in the lower Mississippi River basin comes largely from late summer/fall frontal and convective systems and winter storms. RegCM2 simulated the precipitation climatology reasonably well by capturing major characteristics, such as heavy amounts along the coasts, much less precipitation in the interior United States, and the distinct east-west gradient (Figure 1b). HIRHAM produced annual precipitation climatology similar to RegCM2 and observations (Figure 1c). Overall HIRHAM gave less precipitation than RegCM2 over most of the simulation domain except along the West Coast where HIRHAM's precipitation was 1-2 mm d^{-1} greater. HIRHAM's precipitation pattern agreed better with observations than RegCM2's over the lower Mississippi River basin. Both models captured quite well mountain precipitation such as Colorado upslope and California coastal precipitation as well as orographic precipitation over the Appalachian Mountain range. Such small-scale orographic precipitation is a challenge to present-day GCMs because of their coarse resolution.

One of the most severe RCM deficiencies is the failure to simulate the precipitation maximum in the lower Mississippi Basin. Low values of winter precipitation over the southeastern United States were also found in other RCM and GCM simulations [*Giorgi et al.*, 1994; *Doherty and Mearns*, 1999; *Takle et al.*, 1999]. This precipitation maximum is produced primarily by winter storms originating over the Gulf of Mexico and adjacent coastal regions [*Businger et al.*, 1990], and sea breeze circulations which cannot be resolved by the models. While a comprehensive diagnosis of this deficiency is beyond the scope of this study, a few possible explanations are offered. Comparison with satellite-based precipitation estimates over oceans [*Xie and Arkin*, 1998] suggest that precipitation could be released too early in the models while storms move northeastward from the Gulf of Mexico. Both RCMs simulated high precipitation over the Gulf and weak precipitation inland, suggesting that the model parameterization schemes triggered precipitation too early in the storm life cycle. Our version of RegCM2 omits rainwater as a predictive variable to save computational time so that cloud water rains out immediately with no reevaporation. This would tend to reduce downstream moisture transport.

Underrepresentation of winter storms in forcing boundary conditions could be another reason for the deficiency. The Gulf of Mexico is a data-sparse region where the initial storms might be missed in the NCEP reanalysis. Excluding hurricanes, storms or cyclones originating in the Gulf are typically weaker than midlatitude counterparts. We explored the possibility that boundary influences might lead to low precipitation by extending the simulation domain southward

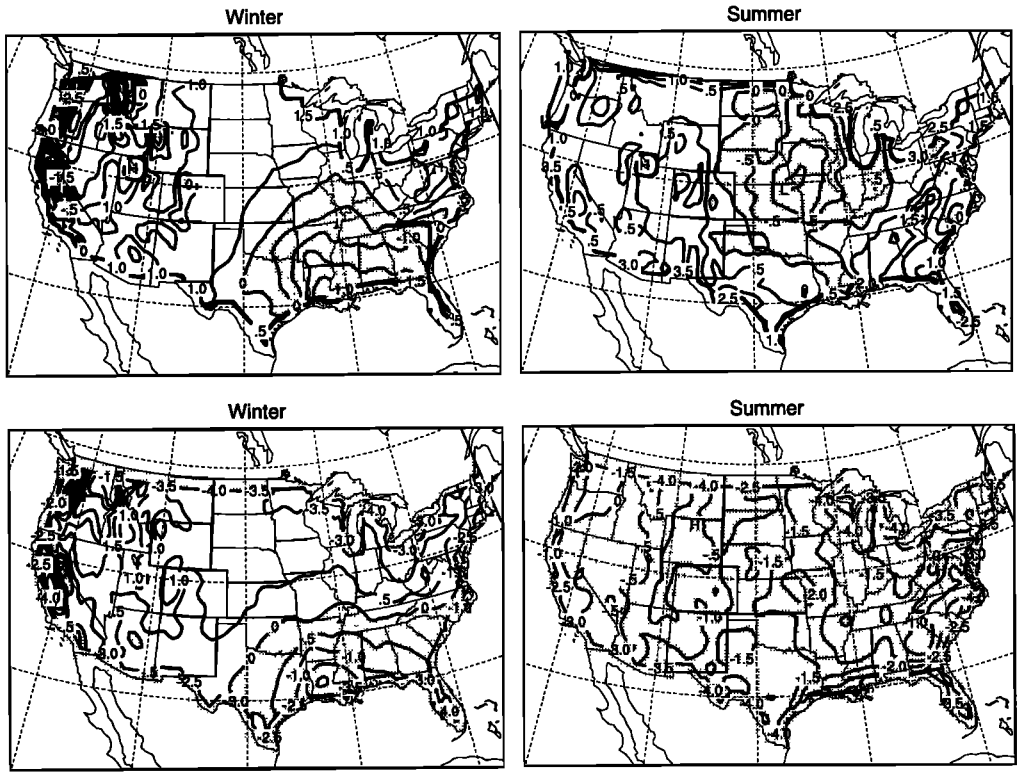

Figure 3. RCM performance bias (simulation - observation) for winter and summer precipitation (mm d^{-1}) averaged over the 10 winters or summers: (top) RegCM2 and (bottom) HIRHAM. Contour interval is 0.5 mm d^{-1}. Negative values are shaded.

by about 1500 km. Running the model for November 1986, when the model had its largest error, did not improve results substantially, suggesting that lateral boundary location is not the cause of the problem.

RegCM2 also simulates excessive precipitation in the western United States, a defect reported by *Giorgi et al.* [1994]. Excessive precipitation is associated with excessive cloud cover in the model and is consistent with the model's underestimation of solar irradiance at the surface [*Pal et al.*, 2000] which is consistently smaller than climatological values by 10-15% [*U.S. Department of Energy*, 1981]. The most frequent daily precipitation in RegCM2 was at about 2.8 mm, whereas observed precipitation occurred at 1.5 mm in the western mountains [K.E. Kunkel, personal communication, 2000]. Intermodel bias for the HADCM2 control driven run has similar patterns in winter but more negative bias in the southeastern United States in summer. Compared to the 1951-1990 climatology, the HADCM2 control climate-driven run oversimulated precipitation in the southeastern United States and Pacific northwest while the model performed well in the central United States, especially capturing the east-west gradient (Figure 2). It should be mentioned that the HADCM2 control climate-driven run simulated 10 years while the observed climatology is for 40 years.

In winter (DJF) the largest RegCM2 positive bias occurs over the Cascade Mountains in central Washington and Oregon where it exceeds 2 mm d^{-1} (Figure 3, top left). This bias could be due in part to the paucity of high-altitude observation stations [*Giorgi and Shields*, 1999]. This positive bias is immediately adjacent to a region of negative bias near the Pacific coast. Such a positive-negative couplet is the typical signal of a phase error, in this case possibly attributable to the use of relatively smooth terrain. Bias magnitude in the central United States is less than 1.0 mm d^{-1}. Summer (JJA) biases have magnitudes mostly within 0.5 mm d^{-1} (Figure 3, top right). However, a negative bias center occurs in the Midwest with peak magnitude exceeding 1.5 mm d^{-1}. The fall bias distribution is similar to spring in the western United States, but bias in the eastern part of the domain is quite different from other seasons, with strong negative bias in the south central United States (not shown).

HIRHAM winter (Figure 3, bottom left) biases are very similar to those of RegCM2, while its summer bias is negative almost everywhere in the domain. The mostly negative summer bias pattern (Figure 3, bottom right) differs from that of RegCM2, possibly because of the differing cumulus parameterization schemes used in the two RCMs. The spring and fall biases in HIRHAM are smaller in magnitude both in the Pacific Northwest and the lower Mississippi basin (not shown).

3.2. Boundary Forcing Bias

The boundary forcing bias for RegCM2 is mostly positive; that is, the simulation driven by HADCM2 current climate gave larger precipitation amounts than the reanalysis driven simulation (Figure 4, top). The largest winter positive bias is located in the southeastern United States where precipitation is mainly associated with winter storms. During summer large positive bias occurs in the central United States and small negative bias occurs in the southwest United States. A possible reason for positive bias is the predominance in summer of convective precipitation, which is sensitive to

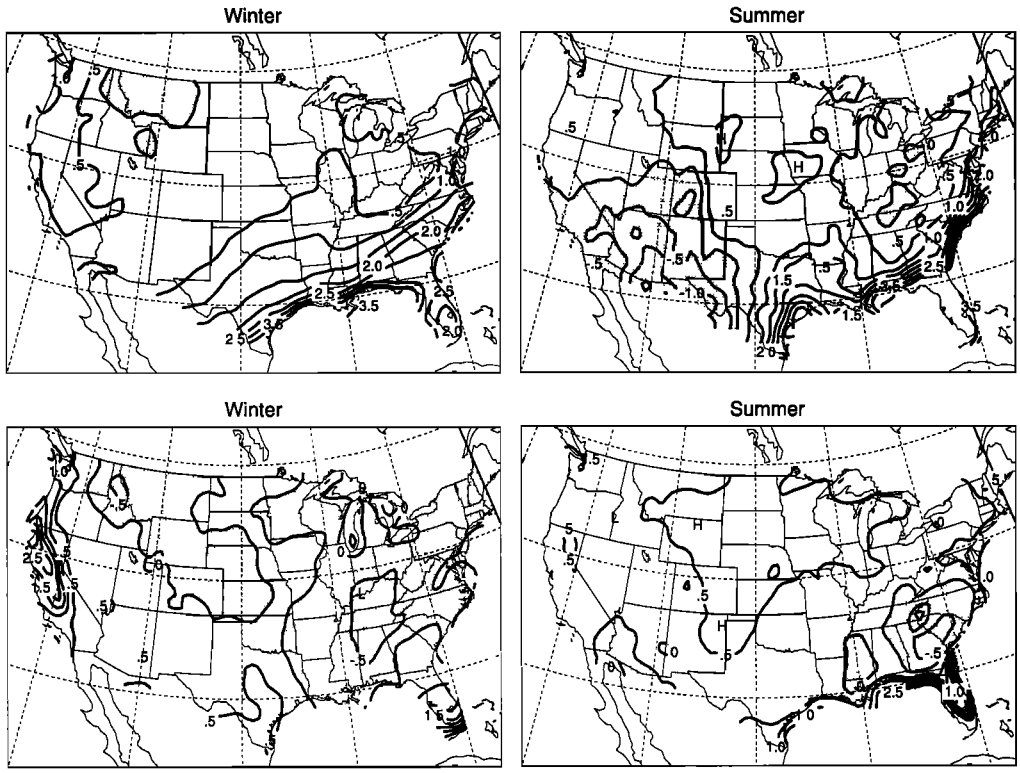

Figure 4. As Figure 3, but for boundary forcing bias (GCM current climate-driven run minus reanalysis-driven run).

subtle differences in forcing [*Crook and Moncrieff*, 1988]. This is especially true over the central United States where mesoscale convective systems produce much of the warm-season precipitation [e.g, *Fritsch et. al.*, 1986]. For both seasons the largest biases occur along the south and east coasts, possibly due to different representations of terrain and coastlines in the RCM and GCM (for example, the Florida peninsula does not exist in the HADCM2 land mask), or the fact that the boundary buffer zone is relatively close to the south and east coasts.

HIRHAM's forcing bias (Figure 4, bottom) is somewhat different from that for RegCM2, with no large positive bias along the south and east coasts as was found in RegCM2. The difference between forcing biases is possibly associated with the different locations and widths of forcing zones. RegCM2 has a smaller domain and wider forcing zone so that the GCM lateral boundary forcing has stronger control on RCM internal performance [see e.g., *Seth and Giorgi*, 1998]. Any forcing difference in NCEP reanalysis and GCM output would show more readily in RegCM2 .

3.3. Intermodel Bias

RegCM2 has more precipitation than HIRHAM for the United States as a whole (Figure 1). Winter intermodel bias (RegCM2 minus HIRHAM) is negative in the western mountains and positive in the east and along the west coast (Figure 5). In summer, RegCM2 simulated larger precipitation amounts than HIRHAM everywhere in the domain. The larger difference in summer could be explained

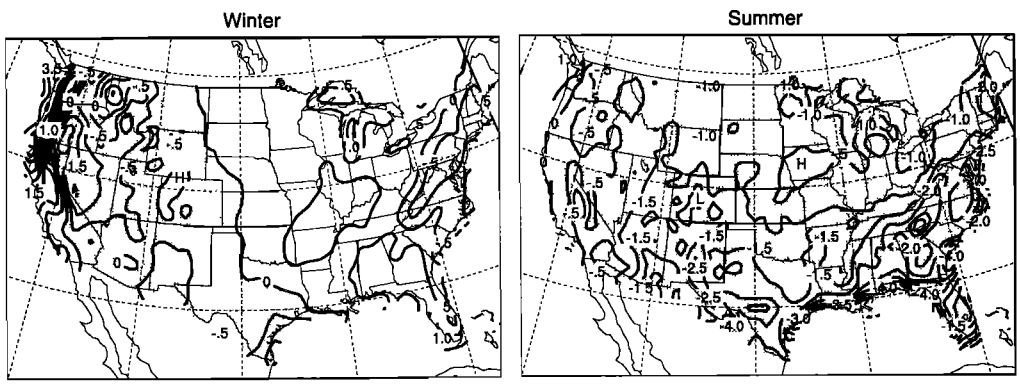

Figure 5. Intermodel bias (HIRHAM run minus RegCM2 run, both driven by reanalysis). Contour interval is 0.5 mm d^{-1}. Negative values are shaded.

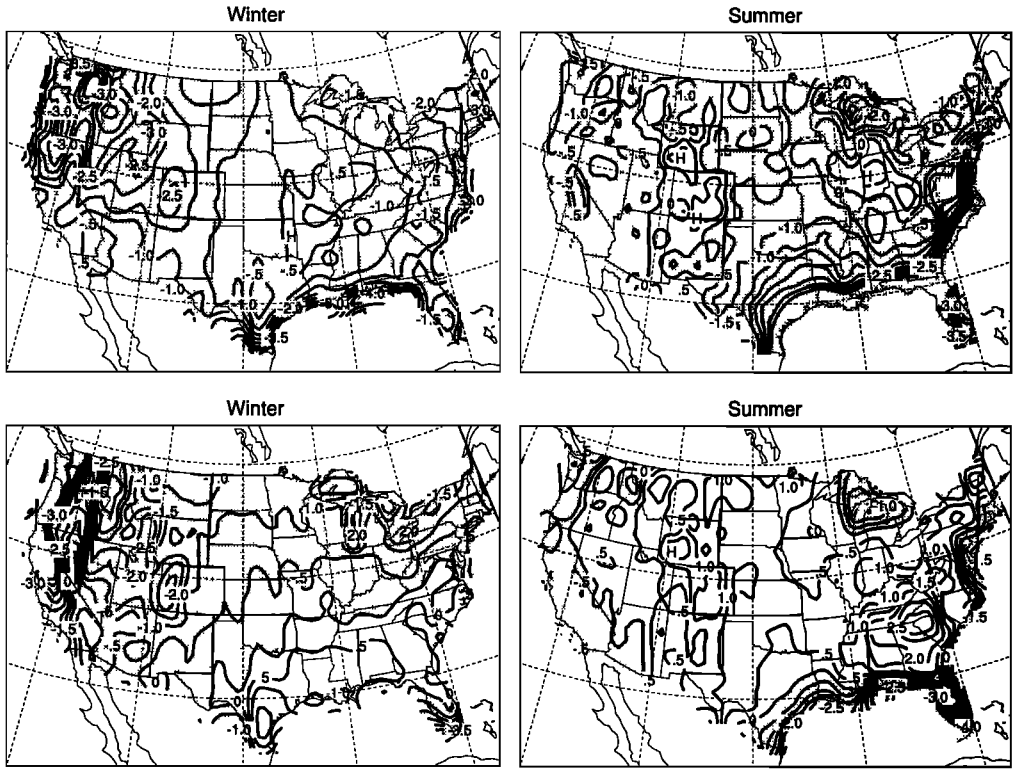

Figure 6. As Figure 3, but for GCM-RCM downscaling bias (GCM's current run minus RCM run driven by GCM's current run).

in part by the differences in cumulus parameterization schemes or by differences in land surface parameters that yield different moisture supply for precipitation. The general pattern of large difference in the south and small in the north is consistent with convection being the main cause for the intermodel bias. Intermodel bias between the two RCMs for the HADCM2 control driven runs is very close to the bias of the NCEP reanalysis-driven runs in summer, but it is large and negative along the south and east coasts in winter (not shown).

3.4. GCM-RCM Downscaling Bias

The GCM-RCM downscaling bias is the precipitation from the HADCM2 control climate run minus precipitation from the RCM run forced by the HADCM2 control climate. The GCM-RCM downscaling bias in RegCM2 is mostly negative across the domain for both summer and winter (Figure 6, top). Especially large negative values occur along the eastern and southern coasts. The GCM-RCM downscaling bias is uniformly small in summer, in contrast to the forcing bias and intermodel bias. HIRHAM GCM-RCM bias shows large negative values in the northwestern United States in winter and positive values in the southeastern United States in summer (Figure 6, bottom).

Combining GCM-RCM downscaling bias with observations (in Figure 1a) shows that the HADCM2 simulation misses much of the orographic precipitation, which might be expected given its coarse resolution. The bias pattern corresponds well with terrain height. The large bias along the Gulf and east coasts may be related to the coarse land-sea mask in HADCM2. The RCM simulated summer precipitation is actually smaller than that from HADCM2 in parts of the interior. This may seem counterintuitive since the former should resolve mesoscale precipitation systems better. However, better resolution of terrain in the RCM will not necessarily lead to larger precipitation in every location. One of the reasons for this is the so-called precipitation shadow downstream of high mountains [*Giorgi et al.*, 1994]. The highest mountain in RegCM2 is 3050 m while it is only about 2100 m in HADCM2. Also RegCM2 resolution distinguishes several mountain ranges, such as the Pacific coast range, the Sierra Nevada, and the Rockies, that HADCM2 lumps into a big hill. This significantly higher terrain can reduce the moisture flux downstream, decreasing precipitation. Lower RCM precipitation also may be attributable to lack of moisture in the GCM lateral boundary conditions due to excessive GCM precipitation upstream from the RCM domain [*Giorgi et al.*, 1994].

3.5. Climate Change

Simulated climate change in precipitation shows distinct differences between summer and winter (Figure 7, top). In winter, precipitation change is positive over the West Coast and northeast states in agreement with *Giorgi et al.* [1994]. Precipitation increase exceeds 2 mm d^{-1} along the West Coast in winter, suggesting more frequent, more moist or stronger winter storms over the eastern Pacific. Winter precipitation decreases along much of the Gulf of Mexico. The simulated precipitation change is small ($\pm$ 0.5 mm d^{-1}) over the central United States. Summer precipitation increase generally is small except for the south-central United States which has a 0.5-1.5 mm d^{-1} increase in precipitation. The relatively modest climate change projected for summer, contrasted with a relatively large intermodel bias during this season, reduces

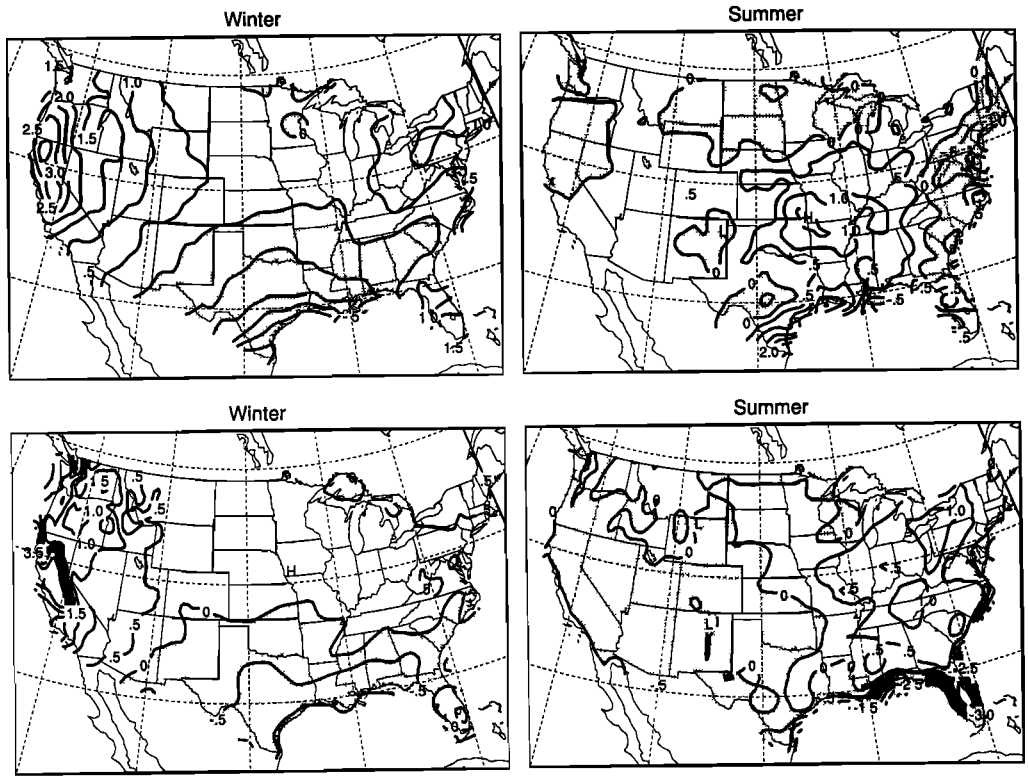

Figure 7. As in Figure 3, but for climate change (GCM scenario-driven run minus control-driven run).

our confidence in summer regional precipitation estimates for future climates. HIRHAM winter change is very similar to RegCM2 (Figure 7, bottom), but its summer change is weaker, especially in the eastern United States. Like RegCM2, its overall change is smallest in summer, but its region of largest increase occurs farther east.

HADCM2 simulated climate changes (Figure 8) for winter revealed an overall distribution similar to those from the two RCMs, with precipitation being controlled by large-scale flow. This is clearly seen in the southeastern United States. However, for the western mountains the maximum precipitation center is shifted eastward of the Cascade Mountains, most likely due to lack of terrain resolution. The HADCM2 projected change in summer precipitation is smaller than the two RCMs; it is even broadly negative in the northwestern United States.

4. Regionalization of Biases and Correlation Analysis

4.1. Seasonal Biases

To regionalize our analysis we divide the continental United States into five regions (Figure 9) based on their climate characteristics, broadly following the Koeppen classification scheme [e.g., *Hidore and Oliver*, 1993]. The first region (Pacific Northwest coast, PNW) has a marine coastal climate. This region has a strong seasonal cycle in precipitation with a winter maximum. The second region (California, CA) has a Mediterranean climate with dry summer and wet winter/spring. The third is the western mountain (MW) region with mostly dry climates. Here the precipitation climatology varies with local topography; most

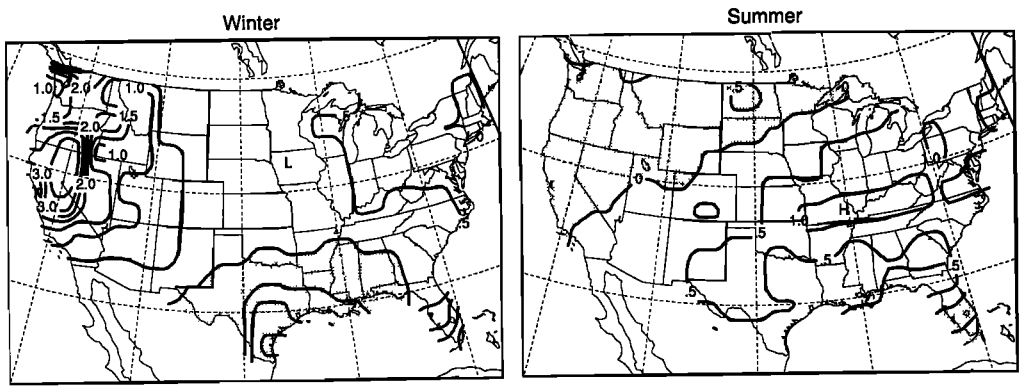

Figure 8. Climate change simulated by HADCM2 in winter and summer precipitation (mm d^{-1}) averaged over the 10 winters or summers. Contour interval is 0.5 mm d^{-1}. Negative values are shaded.

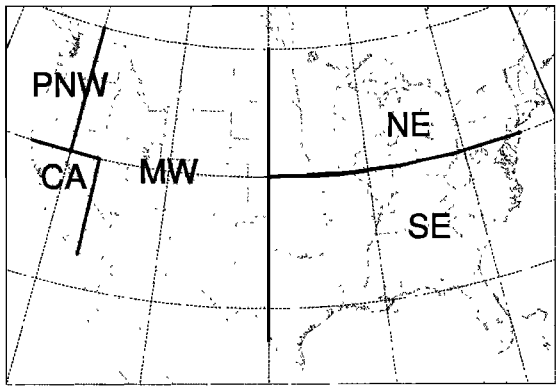

Figure 9. Boundaries of five analysis regions. (See text for region names.)

locations have a weak summer precipitation maximum. The fourth region (northeast United States, NE) has a temperate climate while the fifth region (southeast United States, SE) has a hot and humid climate.

Figure 10 summarizes performance bias, boundary forcing bias, intermodel bias, GCM-RCM downscaling bias, and climate changes for each region and season from RegCM2 simulations. In PNW the model performed well, and the annual model performance bias is only -0.2 mm d^{-1}, a combined result of negative values in winter and fall, and positive values in spring and summer. All biases are large in winter and small in summer, partly because of high precipitation in winter and low precipitation in summer. The positive forcing bias and intermodel bias are quite consistent at around 1.0 mm d^{-1} in all seasons except for summer (about 0.2 mm d^{-1}). GCM-RCM downscaling bias is consistently negative and largest among all biases, including climate change, especially in winter when the magnitude reaches 2.5 mm d^{-1}. Climate change is large and positive, except for summer when it is slightly negative. In CA the bias characteristics are similar to PNW, but with smaller amplitude, especially for the downscaling bias. The MW is characterized by changes that are small in absolute terms but large in relative terms. The changes are seasonally consistent (about 0.5-0.7 mm d^{-1}). The positive RCM performance bias (1 mm d^{-1}) and negative GCM-RCM downscaling bias (-1.6 mm d^{-1}) in winter are the largest in this region. The model has an evident positive performance bias all year around. The forcing bias is very small, possibly because this region is far from the boundary zone so that biases in the driving lateral boundary conditions are minimized and the model internal dynamics predominate. All bias patterns in NE are similar to those in MW despite the difference in geography and topography of the two regions. All absolute biases except the GCM-RCM downscaling bias are small, as is climate change (within 0.4 mm d^{-1}). The results are characterized by large forcing bias in all seasons, varying RCM performance bias and intermodel bias, and medium climate changes.

The bias pattern in SE is different from the other four regions; the largest biases tend to occur in summer, partly because precipitation peaks in late summer/early fall in the region. The forcing bias and GCM-RCM downscaling bias become larger than the other biases, and climate change also is somewhat larger. The large biases appear to be associated with underestimation of moisture fluxes from the Gulf of Mexico (not shown). The forcing bias and GCM-RCM downscaling bias always have opposite signs, meaning that the RCM driven by GCM output has more precipitation compared to the reanalysis driven run, whereas the GCM itself gives noticeably less precipitation. The low precipitation is in part because the GCM would have weaker vertical motion and thus weaker lifting to induce condensation. This occurs in part because topography is smoother and because the GCM coarse resolution does not include mesoscale circulation and vertical motion. In this sense the GCM appears less efficient in producing precipitation than the RCM when both are under similar larger-scale forcing [*Jones et al.*, 1995].

HIRHAM climate change and GCM-RCM downscaling bias in PNW and CA are larger than for RegCM2 (Figure 11). Negative GCM-RCM downscaling bias reaches -3.1 mm d^{-1} in winter. In CA, climate changes are larger than other biases in all seasons (neglecting the very dry summer) with maximum change of 3.6 mm d^{-1} in winter, the largest among all types of biases. HIRHAM, like RegCM2, has small biases and seasonal variations in MW and NE. The largest difference in bias between the two RCMs is in SE where biases and changes are smaller.

Relative biases allow us to compare more clearly regions with different annual precipitation totals. The relative RCM performance bias is normalized by the corresponding observation, whereas the relative forcing bias is normalized by the corresponding RegCM2 simulated value driven by

Table 1. Relative Biases, Differences, and Climate Change in Precipitation for RegCM2

Region	PNW	CA	MW	NE	SE
RCM Performance Bias, % Observation					
Winter	-8	-14	100	49	-15
Spring	4	0	47	21	-6
Summer	13	219	31	-4	15
Fall	-12	-5	55	0	-21
Annual	-5	-6	56	11	-6
Boundary Forcing Bias, % of Reanalysis Driven					
Winter	14	11	12	21	52
Spring	20	2	2	6	29
Summer	19	13	4	19	35
Fall	23	-12	-1	7	37
Annual	18	4	5	13	38
Intermodel Bias, % of RegCM2					
Winter	18	32	-16	13	10
Spring	13	21	-17	0	-5
Summer	-11	-57	-91	-37	-65
Fall	23	19	-39	-4	-5
Annual	16	24	-36	-8	-17
GCM-RCM Downscaling Bias, % of RCM Run					
Winter	-37	-23	-67	-53	-32
Spring	-37	-35	-38	-16	-17
Summer	-42	-60	-10	-21	-48
Fall	-39	-35	-43	-41	-45
Annual	-38	-30	-42	-31	-36
Climate Change, % of Current					
Winter	36	60	29	17	-5
Spring	17	49	28	25	29
Summer	-10	-14	7	1	9
Fall	23	69	27	17	26
Annual	24	56	23	14	14

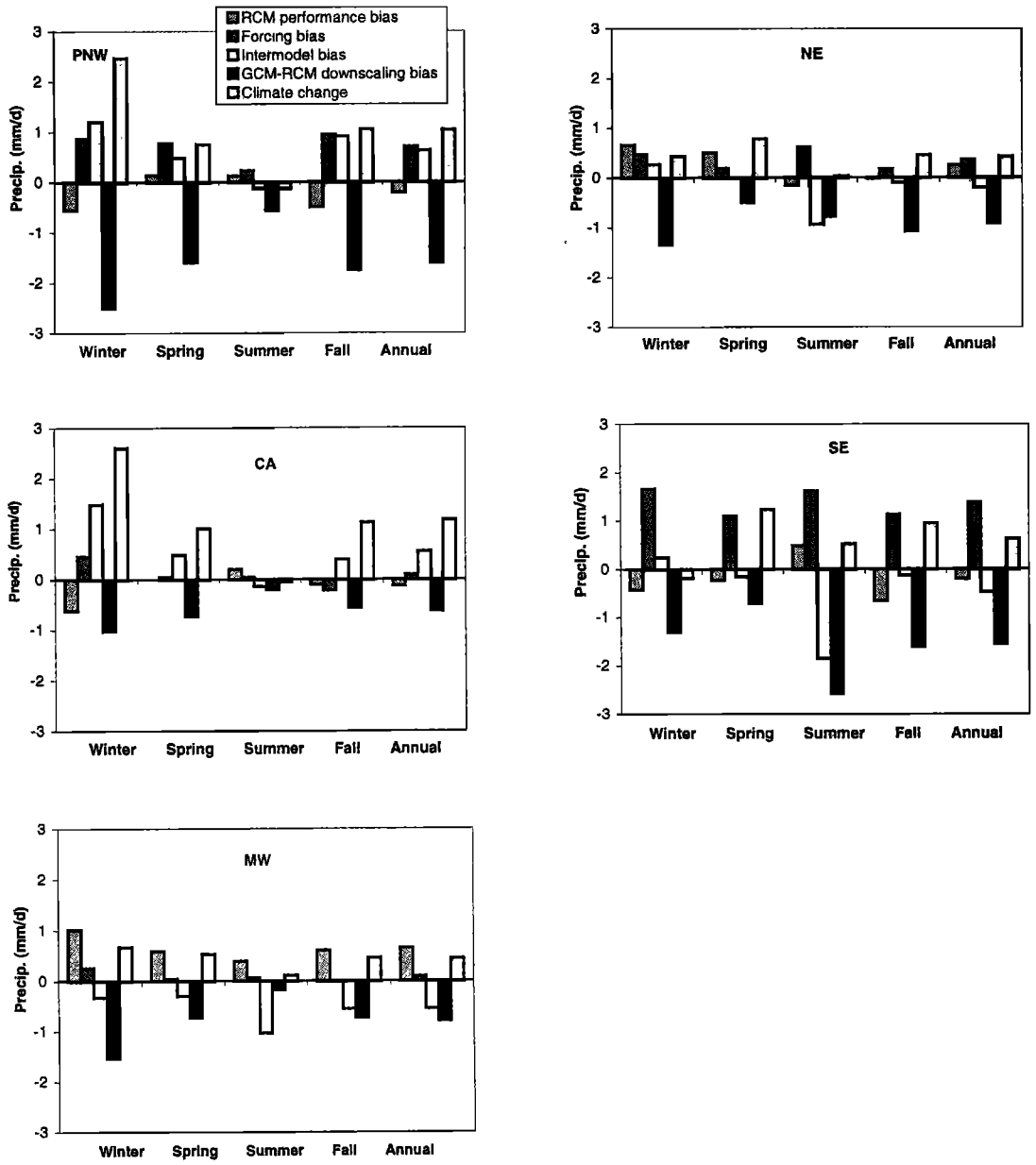

Figure 10. Comparisons of various biases with climate change in seasonal precipitation in different regions for RegCM2.

observations, and so on (see Table 1). The largest annual performance bias (RegCM2) reaches 56% in MW compared with -6% to +11% in other regions. (The high summer bias of 219% can be traced to the very low (0.09 mm d^{-1}) summer precipitation in this region.) The annual boundary forcing bias ranges from +4% in CA to +38% in SE. The intermodel bias is mostly negative (i.e., RegCM2 simulates greater precipitation than HIRHAM), especially in summer. The negative GCM-RCM downscaling bias ranges from 30-42% annually. Annual mean climate change varies from 14% in NE and SE to 56% in CA.

In summary, for RegCM2: (1) Among all types of biases, including climate change, the GCM-RCM downscaling bias is largest, reaching -2.5 mm d^{-1} (-67%) compared with less than $\pm$ 1.5 mm d^{-1} in most other circumstances; (2) among the five regions PNW and SE have largest absolute RCM performance bias, but relative RCM bias is largest in the mountain region (56%, annual), while biases are within $\pm$ 11% in the other four regions; (3) among the four seasons, summer has largest biases but smallest climate change, which lowers our confidence in summer climate projection; and (4) precipitation increase is simulated in most seasons and regions except for the south-central United States summer and east coast winter. The ratio of climate change to various biases is highest along the west coast, while the ratio is lowest in the SE where precipitation is more convective and unresolved sea breeze circulations dominate observed precipitation along the coast [*Sousounis*, 2000].

4.2. Spatial Correlation and Standard Deviation

We calculate spatial correlation coefficients between fields used to compute each bias or change. Table 2 summarizes the correlation coefficients (r) for all regions and seasons. High correlation indicates similar spatial distribution of

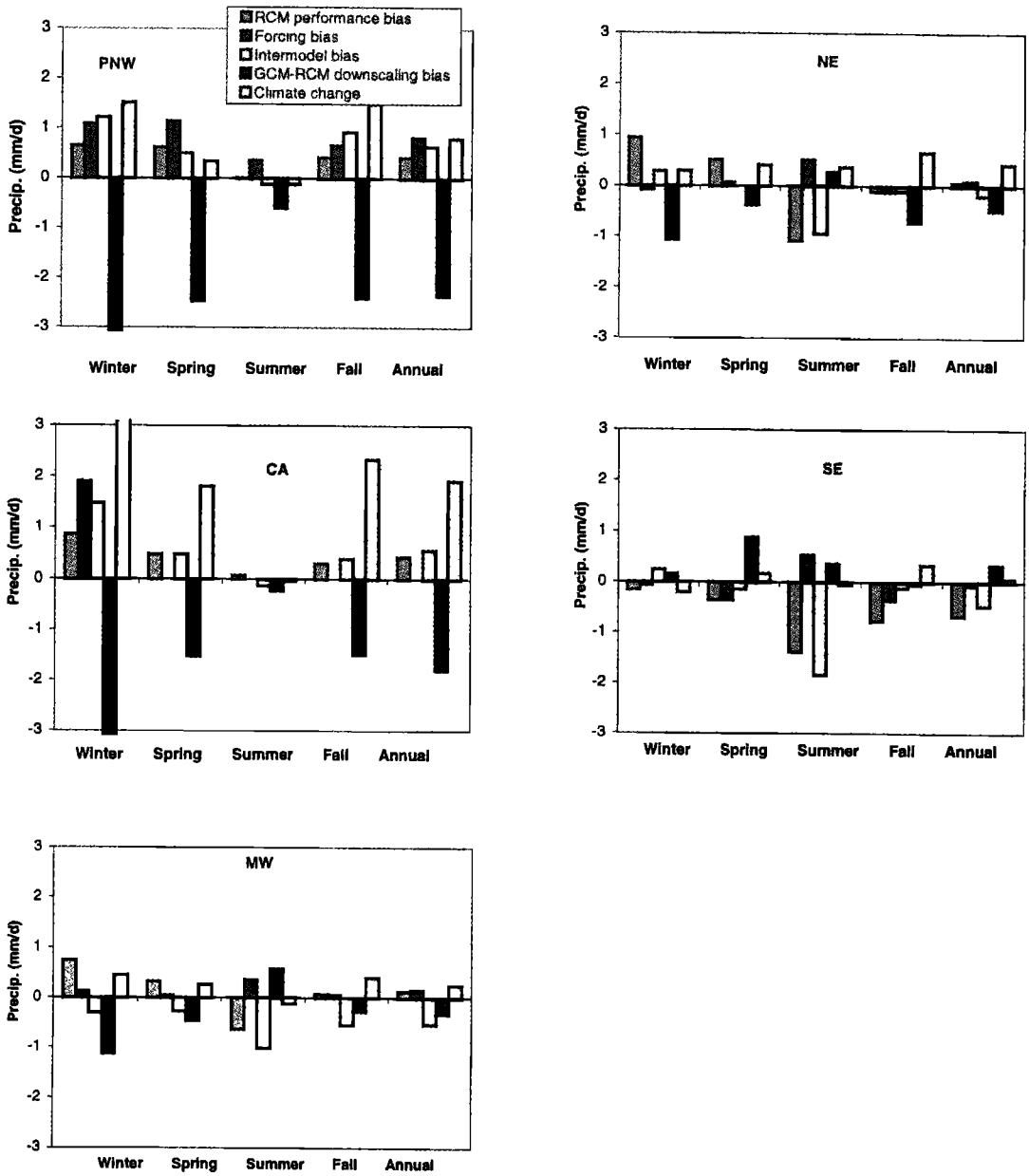

Figure 11. As Figure 10, but for HIRHAM.

precipitation among the different simulation pairs. There is high correlation between the RegCM2 results driven by GCM current and scenario climates (climate change correlation), with all regions having annual $r > 0.85$ (bottom of Table 2). GCMs capture large-scale processes affecting precipitation, monsoonal flows, large-scale orographic lifting, etc., which likely will not change substantially in the near future. So, for instance, it is likely that the western half of the United States will continue to be drier than the eastern half and that moisture originating in the Gulf of Mexico will continue to play a role in precipitation patterns in the southeast United States. Thus even though future precipitation changes, its overall spatial pattern remains relatively similar to the present. The lowest correlation is between modeled and observed precipitation (RCM performance correlation, top of Table 2), reflecting inherent challenges to accurate simulation of precipitation processes. The GCM-RCM correlations are generally low (except CA), a consequence of non-uniform GCM-RCM bias. Among all regions, CA has highest correlation ($r = 0.99$ for climate change), except for RCM performance. This high correlation is the direct manifestation of orographic precipitation where resolving topography well is important.

Spatial standard deviations in the reanalysis-driven run tend to be larger than observed in the west and smaller in the east (Table 3). The model's larger standard deviation in the west may be due in part to the tendency for observing stations to be located at lower elevations, whereas the model precipitation includes high and low elevation points. As expected, spatial standard deviations in the RCM are larger than in the driving GCM, so that the GCM simulation is more spatially uniform than the RCM. The RCM scenario precipitation has more spatial uniformity in summer and stronger spatial heterogeneity in winter than the current climate simulation.

Table 2. Spatial Correlation Coefficients in Precipitation for RegCM2

Region	PNW	CA	MW	NE	SE
		RCM Performance			
Winter	0.40	0.51	0.70	0.94	0.65
Spring	0.34	0.55	0.74	0.85	0.41
Summer	0.58	0.78	0.80	0.40	0.68
Fall	0.47	0.56	0.57	0.84	0.25
Annual	0.38	0.55	0.65	0.87	0.59
		Boundary Forcing			
Winter	0.93	0 98	0.97	0.99	0.72
Spring	0 93	0.99	0 94	0 93	0 29
Summer	0 96	0 98	0 70	0 86	0.87
Fall	0.93	0 99	0 96	0 87	0.91
Annual	0.95	0 99	0.96	0 96	0.85
		Intermodel			
Winter	0 50	0.93	0 91	0.88	0 85
Spring	0 53	0.95	0.85	0.89	0 67
Summer	0.69	-0.08	0.62	0.85	0.80
Fall	0.62	0.85	0.88	0.92	0.68
Annual	0.48	0.90	0.88	0.92	0.74
		GCM-RCM Downscaling Difference			
Winter	0.49	0 80	0 65	0 82	0.80
Spring	0.58	0.88	0 78	0 56	0.04
Summer	0.75	0 82	0.85	0.31	0.31
Fall	0 73	0 93	0.68	0.71	0.55
Annual	0.52	0.88	0.70	0.60	0.39
		Climate Change			
Winter	0.82	0 99	0.96	0 99	0.87
Spring	0.76	0 99	0.88	0 89	0.90
Summer	0 96	0.99	0.96	0.79	0.97
Fall	0.91	0 99	0.96	0.98	0 96
Annual	0.85	0.99	0 93	0 97	0.99

HIRHAM spatial correlation coefficients are generally larger than RegCM2's, especially in PNW, where HIRHAM's highest (0.85, annual) and RegCM2's lowest (0.38) RCM correlations occur. The other types of correlations are comparable between the two models (not shown).

4.3. Climate Change Versus Biases

We computed the ratio of climate change to the largest in magnitude of RCM performance bias (ΔP_{RCM}), boundary forcing bias (ΔP_{forc}), and intermodel bias (ΔP_{imd}), for each region and season, that is,

$$R_{\mathrm{chng}} = \frac{\left|\Delta P_{\mathrm{chng}}\right|}{\max\left(\left|\Delta P_{RCM}\right|, \left|\Delta P_{\mathrm{forc}}\right|, \left|\Delta P_{\mathrm{imd}}\right|\right)}. \quad (4)$$

There may be other biases (such as if we had two GCMs giving different precipitation for the current climate) that might further influence R_{chng}, so the confidence level suggested by R_{chng} is relative to the suite of biases used in its definition. We did not include GCM-RCM downscaling bias in (4) since it does not necessarily imply error in RCM simulation. Various measures could be used to compare climate change with the magnitude of simulation deficiency. Model deficiencies are often assumed to be reduced when estimating climate change by taking differences of the two simulations (e.g., if the model has a warm bias, it is assumed to be biased both for the current climate and future scenario climate). Although a sum or mean of biases is a possible measure for comparison with climate change, we view the present choice as conservative in comparison with bias-cancellation assumptions conventionally used for interpreting climate change. Large R_{chng} should be interpreted as a necessary rather than sufficient condition for reliable climate change projection. Within these limitations, while comparing R_{chng} of different regions within a given simulation, confidence in the simulated climate change increases as R_{chng} increases. Conversely, we have less confidence in changes when R_{chng} is small.

The climate change ratio is substantially larger than 1 in several seasons and regions (Figure 12). We see that summer values of R_{chng} are always less than 1 and CA has large R_{chng} (except for summer). HIRHAM R_{chng} values are generally similar to RegCM2's. For most regions both models tend to have large R_{chng} for spring and fall, somewhat smaller values for winter, and $R_{\mathrm{chng}} < 1$ for summer. This consistency between the models suggests that changes to summer precipitation pose the greatest challenge to regional climate modeling over the United States.

We also counted the number of times when R_{chng} is greater than 1 (Table 4). Confidence in a change is presumed to be greater when the change exceeds bias magnitudes most frequently. Especially noteworthy are seasons and regions where results from both regional models indicate high confidence in the simulated changes. Table 4 shows that

Table 3. Standard Deviation Biases in Precipitation (mm d^{-1}) Between Different Simulations for RegCM2

Region	PNW	CA	MW	NE	SE
		RCM Performance			
Winter	2.60	0.98	-0.25	-0.14	0.31
Spring	1.24	0.24	0.05	-0.01	0.21
Summer	0.03	-0.11	0 01	-0 27	-0.27
Fall	1.58	0 48	-0 08	0.04	-0.23
Annual	1.40	0 41	-0.05	-0.14	-0.03
		Boundary Forcing			
Winter	0 02	0.16	0.01	0.22	0 76
Spring	0 18	0.13	0.06	0 11	0.43
Summer	0.03	0.10	0 22	0.04	1.16
Fall	0.49	0.01	0 23	0 37	1.27
Annual	0 16	0.10	0.12	0.19	0 93
		Intermodel			
Winter	1.46	0.45	0 00	-0.15	-0.02
Spring	0.57	0.07	0 14	-0.19	0.30
Summer	0.06	-0.08	-0.28	-0.22	-0.78
Fall	0 89	0.28	0.09	0.02	-0.37
Annual	0.74	0.17	0.10	-0.12	-0.19
		GCM-RCM Downscaling Difference			
Winter	0.34	-0.35	-0.30	-0.49	-0.75
Spring	-0.12	-0.22	-0.09	-0.04	-0 10
Summer	-0.10	-0.14	0.04	-0.04	-1.52
Fall	-0.31	-0.15	-0.25	-0.44	-1.59
Annual	-0.13	-0.22	-0.20	-0.31	-1.14
		Climate Change			
Winter	0.40	0.43	0.59	0 38	0.01
Spring	-0.02	0.21	0 15	0 20	0.49
Summer	0.05	-0.09	-0.07	-0 09	-0.03
Fall	-0.25	0.33	0.19	-0.05	0.20
Annual	-0 05	0.22	0.17	0 08	0.16

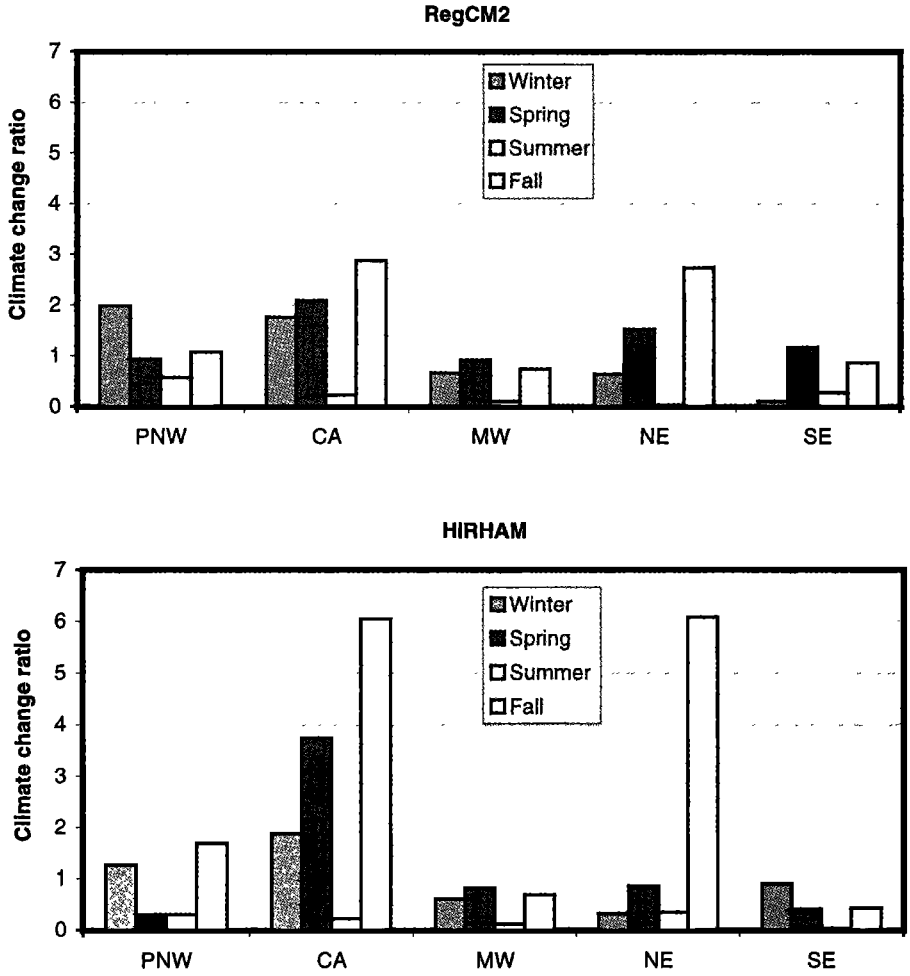

Figure 12. The climate change ratio (change divided by maximum bias) in different seasons and regions: (top) RegCM2 and (bottom) HIRHAM.

greatest confidence can be given to change in CA, which in both models exceeds all biases in all seasons except summer. The models also indicate higher confidence in fall changes for PNW and NE and in winter changes for PNW. Furthermore, both models indicate low confidence in summer change for all regions and low confidence any time of year for changes in MW and SE. Overall, the two models' counts of climate change exceeding bias are within ± 1 of each other for every season and region (25 cases) except PNW and SE in spring.

Table 4. Number of Biases Less Than Climate Change

Region	PNW	CA	MW	NE	SE
		RegCM2			
Winter	3	3	2	1	0
Spring	2	3	2	3	3
Summer	2	1	1	0	1
Fall	3	3	1	3	2
Annual	3	3	1	3	2
		HIRHAM			
Winter	3	3	2	2	2
Spring	0	3	1	2	1
Summer	2	0	0	0	0
Fall	3	3	2	3	1
Annual	3	3	2	3	1

The models thus demonstrate substantial consistency in the depiction of changes.

We close this section with a simple significance test. Using a t-test with 2x10 years of simulations, we examine the projected precipitation increases for statistical significance, given two means and variances. In most of the continental United States, the t-value for annual mean precipitation exceeds 6 (not shown), which is much larger than the 95% confidence level, 1.73. RCM simulated climate change in annual precipitation is thus statistically significant. There are only two locations where the simulated precipitation increase is not statistically significant according to this simple test: areas in Texas and New Mexico and northern Minnesota, presumably a result of relatively weak precipitation increase.

5. Summary and Discussion

Regional climate model (RCM) simulation is relatively new compared to global climate model (GCM) simulation and thus some aspects of RCM simulations are not rigorously tested. A reliable regional climate projection can be obtained only if sources of uncertainties are carefully examined. For example, intermodel comparison among RCMs, although addressed in a few studies, has not been as extensive as for global models (e.g., the Atmospheric Model Intercomparison Project [*Gates*

et al., 1999]). Furthermore, nested RCM simulation is in large part a lateral boundary problem, so that the quality of lateral boundary forcing plays an important role in RCM simulations. Most previous regional climate studies have used a single model, one source of boundary forcing and short integration periods (a few months to years). Under these circumstances identifying causes of differing climate changes is difficult if not impossible [*Leung and Ghan*, 1999]. Furthermore, most of published regional climate projection studies over the United States have been based on $2xCO_2$ equilibrium GCM simulations, which tend to predict greater climate changes compared to transient scenario integrations at the time of CO_2 doubling.

To systematically address these issues, we have used two regional climate models (RegCM2 and HIRHAM) forced by three sets of lateral boundary conditions to produce six 10-year climate simulations for the continental United States at about 50-km horizontal grid spacing. Driven by common boundary conditions, the two RCMs produced similar overall patterns in precipitation, although they differed in the details of their spatial and seasonal distribution. Common precipitation climatology features simulated by both models included realistic orographic precipitation, east-west transcontinental gradients, and reasonable annual cycles over different geographic locations. However, both models missed heavy cool-season precipitation in the lower Mississippi River basin, a seemingly common model defect.

Spatial correlation coefficients of precipitation were computed between simulation pairs in the 2x3 set. The climate change correlation is highest and the RCM performance correlation is lowest while boundary forcing and intermodel correlations are intermediate. The high spatial correlation for climate change suggests that even though future precipitation is projected to increase, its overall continental-scale spatial pattern is expected to remain relatively constant. The low RCM performance correlation shows a modeling challenge to reproduce observed spatial precipitation patterns.

Projected precipitation changes are positive over most areas during all seasons except winter near the Texas and south coast. The annual relative increase is 14-56% depending on the region. The dry west has larger increases than the wet east in both relative and absolute terms. While agreeing with typical GCM simulations in terms of general distribution and seasonality, the RCMs examined here provide more spatial variability, especially in mountainous areas. The GCM-RCM downscaling bias is by far the largest among all biases including climate change, implying potential for RCMs to improve upon GCM simulations. The bias analysis shows that (1) climate change is substantially larger than the largest biases in several seasons and regions; (2) summer ratios of climate change versus bias are always less than 1; and (3) the ratio of climate change to bias is especially large in the California region.

The differences between the suite's runs indicate where improvements in modeling or understanding of model behavior are most needed in order to improve confidence in climate change projections. For example, boundary forcing bias is large for all seasons in the southeastern United States. Since the RCM (performance) bias for this region is relatively small, reducing forcing bias requires that the GCM provide more realistic boundary values for RCMs. For the two regions along the West Coast, intermodel bias is relatively large, implying that improvements in RCM modeling are important for increasing confidence as well as consistency in projected climate change. The West Coast intermodel bias is largest in winter, suggesting that RCM interaction between onshore flow and topography needs improvement. The GCM-RCM downscaling bias is consistently large. Better resolved topography by the RCM compared to the GCM may mean that the RCM is simulating topographic precipitation more accurately, so that the bias represents an improvement in regional precipitation simulation. The relatively small RCM performance bias compared to GCM-RCM downscaling bias in the Pacific Northwest is a case in point.

Finally, it should be mentioned that the projected climate change in this study was specifically based on a scenario climate around 2040-2049 and our results could differ for other future periods or other assumed scenarios. Like other modeling studies, the results of this study could differ if other GCMs or RCMs were used [*Roeckner et al.*, 1999, *Doherty and Mearns*, 1999]. Employing a larger set of RCMs, larger simulation, and comparisons among different GCMs could better define the general applicability of our results.

Acknowledgments. This is journal paper J-19378 of the Iowa Agriculture and Home Economics Experiment Station. The computer resources used for the RegCM2 simulations in this study were provided by the NCAR CSL facility. The computer resources used for HIRHAM were provided by the Danish Meteorological Institute. The Electric Power Research Institute, California Energy Commission, and U S National Oceanic and Atmospheric Administration (grant NA86GP0572) provided financial support for this project. We are grateful to Filippo Giorgi and Christine Shields for consultation on RegCM2, and David Hassell and Richard Jones of the Hadley Centre, who kindly provided HADCM2 outputs. We also thank Philippe Lopez for assistance on setting up and running the HIRHAM model for the U S. domain Finally we are thankful to anonymous reviewers of this paper

References

Arakawa, A , and W.H. Schubert, Interaction of a cumulus cloud ensemble with the large-scale environment, *J Atmos Sci , 31*, 674-701, 1974

Briegleb, B P , Delta-Eddington approximation for solar radiation in the NCAR community climate model, *J Geophys Res., 97*, 7603-7612, 1992.

Businger, S , D.I Knapp, and G.F Watson, Storm following climatology of precipitation associated with winter cyclones originating over the Gulf of Mexico, *Weather Forecasting, 5*, 378-403, 1990.

Christensen, J.H., O.B. Christensen, P. Lopez, E. van Meijgaard, and M. Botzet, The HIRHAM4 Regional Atmospheric Climate Model, *DMI Sci.. Rep. 96-4*, Dan. Meteorol. Inst , Copenhagen 1996.

Christensen, J H., B. Machenhauer, R.G. Jones, C. Schär, P.M. Ruti, M Castro, and G. Visconti, Validation of present-day regional climate simulations over Europe: LAM simulations with observed boundary conditions, *Clim Dyn , 13*, 489-506, 1997.

Christensen, O.B , J.H. Christensen, B. Machenhauer, and M. Botzet, Very high-resolution regional climate simulations over Scandinavia. Present climate, *J. Clim., 11*, 3204-3229, 1998.

Cress, A., D Majewski, D.R. Podzun, and V Renner, Simulation of European climate with a limited area model, I, Observed boundary conditions, *Beitr. Phys. Atmos., 68*, 161-177, 1995.

Crook, N. A., and M. W. Moncrieff, The effect of large-scale convergence on the generation and maintenance of deep moist convection, *J. Atmos Sci., 45*, 3606-3624, 1988.

Cubasch, U., H. von Storch, J. Waszkewitz, and E. Zorita, Estimates of climate change in southern Europe derived from dynamical climate model output, *Clim. Res , 7*, 129-149, 1996.

Davies, H.C , and R.E. Turner, Updating prediction models by dynamic relaxation: An examination of the technique, *Q.J.R. Meteorol. Soc , 103*, 225-245, 1977.

Dickinson, R.E., R.M. Errico, F. Giorgi, and G T. Bates, A regional climate model for the western United States, *Clim. Change, 15*, 383-422, 1989.

Dickinson, R.E., A. Henderson-Sellers, and P.J. Kennedy, Biosphere-atmosphere transfer scheme (BATS) version 1e as coupled to NCAR community climate model, *NCAR Tech. Note 387+STR*, 72 pp., Natl. Cent. for Atmos Res., Boulder, Colo , 1992.

DKRZ, The ECHAM-3 atmospheric general circulation model, *DKRZ Tech. Rep. No. 6*, 186 pp., Hamburg, Germany, 1992.

Doherty, R., and L.O. Mearns, A comparison of simulations of present climate from two coupled atmospheric-ocean GCMs against observations and evaluation of their future climates. Report to the NIGEC National Office, 47 pp., Natl. Cent. for Atmos. Res., Boulder, Colo, 1999.

Dümenil, L., and E. Todini, A rainfall-runoff scheme for use in the Hamburg climate model, in *Advances in the Theoretical Hydrology*, vol. 1, *EGS Series of Hydrological Sciences*, pp 129-157, Elsevier Sci., New York, 1988.

Fritsch, J.M., R.J. Kane, and C.R. Chelius, The contribution of the mesoscale convective weather systems to the warm-season precipitation of the United States, *J. Clim. Appl. Meteorol, 25*, 1333-1345, 1986.

Gates, W.L., et al., An overview of the results of the atmospheric model intercomparison project. *Bull. Am Meteorol. Soc., 80*, 29-55, 1999.

Giorgi, F., and C. Shields, Tests of precipitation parameterizations available in the latest version of the NCAR regional climate model (RegCM) over the continental U S., *J. Geophys Res., 104*, 6,353-6,376, 1999.

Giorgi, F., M.R. Marinucci, and G. Visconti, A $2xCO_2$ climate change scenario over Europe generated using a Limited Area Model nested in a General Circulation Model 2, Climate change scenario. *J. Geophys. Res., 97*, 10,011-10,028, 1992.

Giorgi, F., M.R. Marinucci, G T. Bates, and G. De Canio, Development of a second-generation regional climate model (RegCM2), I, Boundary-layer and radiative transfer, *Mon Weather Rev., 121*, 2794-2813, 1993a.

Giorgi, F, M.R Marinucci, G T Bates, and G. De Canio, Development of a second-generation regional climate model (RegCM2), II, Convective processes and assimilation of lateral boundary conditions. *Mon. Weather Rev., 121*, 2814-2832, 1993b.

Giorgi, F., C. Shields, and G T Bates, Regional climate change scenario over the United States produced with a nested regional climate model, *J. Clim., 7*, 375-399, 1994.

Giorgi, F, L.O., Mearns, C. Shields, and L. McDaniel, Regional nested model simulations of present day and $2xCO_2$ climate over the Central Plains of the U.S., *Clim. Change, 40*, 457-493, 1998.

Grell, G.A., Prognostic evaluation of assumptions used by cumulus parameterizations, *Mon. Weather Rev , 121*, 764-787, 1993.

Hidore, J.J., and J.E. Oliver, *Climatology: An Atmospheric Science*, Macmillan, Old Tappan, N. J., 1993.

Hirakuchi, H., and F. Giorgi, Multi-year present day and 2xCO2 simulations of monsoon climate over Asia and Japan with a regional climate model nested in a general circulation model, J. *Geophys. Res., 100*, 21,105-21,126, 1995.

Holtslag, A.A.M., E.I.F. de Bruijn, and H.L. Pan, A high resolution air mass transformation model for short-range weather forecast, *Mon. Weather Rev., 118*, 1561-1575, 1990.

Hong, S.-Y., and H.-M.H. Juang, Orography blending in the lateral boundary condition of a regional model, *Mon. Weather Rev., 126*, 1714-1718, 1998.

Houghton, J.T., L.G. Meria Filho, B A. Callander, N. Harrris, A. Kattenberg, and K. Maskell (Eds), *Climate Change 1995: The Science of Climate Change*, 572 pp., Cambridge Univ. Press, New York, 1996.

Hsie, E.-Y., R.A. Anthes, and D. Keyser, Simulations of frontogenesis in a moist atmosphere using alternative parameterizations of condensation and precipitation, *J. Atmos. Sci., 41*, 2701-2716, 1984.

Johns, T.C., R.E. Carnell, J.F. Crossley, J.M. Gregory, J.F B. Mitchell, C.A. Senior, S.F.B. Tett, and R.A. Wood, The second Hadley Centre coupled occean-atmosphere GCM: model description, spinup, and validation, *Clim Dyn., 13*, 103-134, 1997.

Jones, R.G., J.M. Murphy, and M. Noguer, Simulation of climate change over Europe using a nested regional-climate model. I, Assessment of present climate, including sensitivity to location of boundaries *Q.J.R.. Meteorol. Soc., 121*, 1413-1450, 1995.

Källén, E., HIRLAM documentation manual, system 2 5, 126 pp., Swed. Meteorol. and Hydrol. Inst., Norrkoping, 1996.

Kalnay, E , et al., The NCEP/NCAR 40-Year Reanalysis Project, *Bull. Am. Meteorol. Soc., 77*, 437-471, 1996.

Karl, T.R., W.-C. Wang, M.E. Schlesinger, and R.W. Knight, A method of relating general circulation simulated climate to the observed local climate, I, Seasonal statistics, *J. Clim., 3*, 1053-1079, 1990.

Kittel, T G F., N A. Rosenbloom, T.H. Painter, D.S. Schmiel, and VEMAP modeling participants, The VEMAP integrated database for modeling United States ecosystem/vegetation sensitivity to climate, *J Biogeogr , 22*, 857-862, 1995

Leung, L.R., and S.J. Ghan, Pacific Northwest climate sensitivity simulated by a regional climate model driven by a GCM, I, Control simulations, *J. Clim , 12*, 2010-2030, 1999.

Leung, L.R., S.J. Ghan, Z.-C. Zhao, Y. Luo, W.-C. Wang, and H.-L. Wei, Intercomparison of regional climate simulations of the 1991 summer monsoon in eastern Asia, *J. Geophys. Res., 104*, 6425-6454, 1999

Machenhauer, B , M. Windelband, M. Botzet, J.H. Christensen, M. Déqué, R.G. Jones, P.M Ruti, and G. Visconti, Validation and analysis of regional present-day climate and climate simulations over Europe, *MPI Rep. 275*, Max-Planck-Inst., Hamburg, Germany, 1998

McGregor, J.L., and K. Walsh, Climate change simulations of Tasmanian precipitation using multiple nesting, *J. Geophys. Res., 99*, 20,889-20,905, 1994.

Pal, J.S, E.E. Small, and A.B Eltahir, Simulation of regional scale water and energy budgets: Representation of subgrid cloud and precipitation processes within RegCM, *J. Geophys. Res., 105*, 29,579-29,594, 2000

Podzun, R , C.D. Majewski, and V. Renner, Simulation of European climate with a limited area model, I, A GCM boundary conditions, *Beitr Phys. Atmos., 68*, 178-225, 1995.

Roeckner, E , et al., The atmospheric general circulation model ECHAM-4: Model description and simulation of present-day climate, *MPI Rep 218*, Max-Planck-Inst., Hamburg, Germany, 1996.

Roeckner, E , L. Bengtsson, J. Feichter, J. Lelieveld, and H. Rodhe, Transient climate change simulations with a coupled atmosphere-ocean GCM including the tropospheric sulfur cycle, *J. Clim.*, 12, 3004-3032, 1999.

Semazzi, F.H.M, N.-H. Lin, Y. -L. Lin, and F. Giorgi, A nested model study of the Sahelian climate response to sea-surface temperature anomalies, *Geophys. Res. Lett., 20*, 2897-2900, 1993.

Seth, S., and F. Giorgi, The effects of domain choice on summer precipitation simulation and sensitivity in regional climate simulation, *J. Clim., 11*, 2698-2712, 1998

Simmons, A., and D.M. Burridge, An energy and angular momentum conserving vertical finite difference scheme and hybrid vertical coordinates, *Mon. Weather Rev., 109*, 758-766, 1981.

Sousounis, P J , A synoptic assessment of climate change model output: Explaining the differences and similarities between the Canadian and Hadley climate models; paper presented at 11th Symposium on Global Changes Studies, Am. Meteorol. Soc., Jan. 9-14, 2000.

Sundqvist, H., A parameterization scheme for non-convective condensation including prediction of cloud water content, *Q.J.R. Meteorol. Soc., 104*, 677-690, 1978.

Takle, E.S., et al., Project to Intercompare Regional Climate Simulations (PIRCS): Description and Initial results, *J. Geophys. Res., 104*, 19,443-19,461, 1999.

Tett, S.F.B., T.C. Johns, and J.F B. Mitchell, Global and regional variability on a coupled AOGCM, *Climate Dyn., 13*, 303-323, 1997.

Tiedtke, M., A comprehensive mass flux scheme for cumulus parameterization in large-scale models. *Mon. Weather Rev., 117*, 1179-1800, 1989.

U.S Department of Energy, Solar Radiation Energy Atlas of the U.S. SERI/SP-642-1037, 167 pp , U.S. Gov. Print. Off., Washington, D. C., 1981.

Xie, P., and P.A. Arkin, Global monthly precipitation estimates from

satellite-based outgoing longwave radiation, *J. Clim., 11*, 137-164, 1998.

Zortia, E., J.P. Hughes, D.P. Lettenmaier, and H. von Storch, Stochastic characterization of regional circulation patters for climate model diagnosis and estimation of local precipitation, *J. Clim., 8*, 1023-1042, 1995.

R.W. Arritt, W.J. Gutowski, Z. Pan, and E.S. Takle, Department of Agronomy, Iowa State University, 3010 Agronomy Hall, Ames, IA 50011. (panz@iastate.edu)

J.H. Christensen, Danish Meteorological Institute, Lyngbyvej 100, DK-2100 Copenhagen Ø, Denmark.

F. Otieno, Department of Geological and Atmospheric Sciences, Iowa State University, Ames, IA 50011.

(Received September 29, 2000; revised March 19, 2001; accepted March 27, 2001.)